Damage Tolerance of Wrought Alloy 718 Ni-Fe-Base Superalloy

M. Chang, A.K. Koul, P. Au, and T. Terada

The influence of a modified heat treatment (MHT) and the standard heat treatment (SHT) on the damage tolerance of alloy 718 turbine disk material has been studied over a range of temperatures—from room temperature to 650 °C. The influence of these heat treatments on creep, low-cycle fatigue (LCF), notch sensitivity, cyclic stability, and fatigue crack growth rate (FCGR) properties has been studied. The microstructure developed through the MHT sequence is shown to be damage tolerant over the temperature range studied. Shot peening leads to a marked improvement in the LCF crack initiation life of the MHT material relative to the SHT material at 650 °C. Serrated grain boundaries formed through controlled precipitation of grain-boundary δ phase are beneficial to elevated-temperature FCGRs. The δ-phase precipitates formed at an angle to the grain boundaries do not make the material notch sensitive.

1. Introduction

A DAMAGE-TOLERANT microstructural design philosophy for turbine disk materials has been developed by Koul et al. (Ref 1) in which microstructures are designed to reduce elevated-temperature creep and fatigue crack growth rates (CCGRs and FCGRs) with minimal loss in low-cycle fatigue (LCF) crack initiation life. A number of other workers have recently used these microstructural design concepts to improve the damage tolerance of powder metallurgy turbine disk materials, such as René (Teledyne Allvac/Vasco, Monroe, NC) 88DT and N18 (Ref 2, 3).

Previously, a damage-tolerant microstructure was developed for alloy 718 turbine disk material by using a modified heat treatment (MHT) to demonstrate the viability of the microstructural design concepts described in Ref 1. The MHT produces a coarser grain size relative to the standard heat treatment (SHT), and it also produces a serrated grain-boundary structure through controlled precipitation of needlelike δ phase at the grain boundaries. A coarse grain size and the presence of serrations are expected to suppress grain-boundary sliding, and the serrations are also expected to make the crack path more tortuous. Previous test results at 650 °C showed that, compared to the SHT, the MHT substantially decreased the FCGRs and CCGRs of alloy 718 and improved the cyclic stability of the material (Ref 1). However, the relative contributions of a coarse grain size and serrated grain boundaries toward improved crack growth resistance were not studied in these investigations. The benefit to FCGRs through MHT was also

accompanied by a small reduction in LCF crack initiation life at 650 °C. It has been suggested that the loss in LCF life in alloy 718 subjected to MHT occurs due to its lower yield strength and the presence of a larger grain size (Ref 1, 4, 5). It has been argued, however, that a large number of aeroengine rotating components, including turbine disks, are shot peened prior to use and that, relative to the SHT material, shot peening would introduce a larger residual compressive stress zone in the MHT material due to its lower yield strength (Ref 6). This is expected to improve LCF crack initiation life, but the hypothesis has not been verified experimentally.

Apart from a small loss in LCF life, concern has always been expressed regarding the notch sensitivity of the damage-tolerant microstructure owing to the presence of grain-boundary δ phase. Sjoberg, Ingesten, and Carlson (Ref 7) have conducted a thorough literature review on the correlation between the presence of grain-boundary δ phase and the notch sensitivity of alloy 718. They suggest that, although opinions differ on the notch sensitivity of alloy 718, the orientation of δ-phase needles relative to the grain-boundary plane appears to be a controlling factor. The δ-phase needles precipitated along the grain boundaries render the material notch sensitive, whereas δ-phase needles precipitated at an angle to the grain-boundary plane and protruding into the grains do not make the material notch sensitive. This phenomenon obviously needs further investigation.

A turbine disk is always subjected to radial temperature variations; the bore regions may be exposed to temperatures as low as 150 °C, the bolt hole regions may be exposed to intermediate temperatures on the order of 500 to 550 °C, and the rim may be subjected to temperatures as high as 600 to 700 °C. In this article, the LCF and FCGR properties of the standard and damage-tolerant microstructures of alloy 718 are compared over a range of temperatures between room temperature and 650 °C. Creep properties of the two microstructures are also compared at 650 °C, because creep life is an essential design feature for the disk rim region. Finally, the issues relating to the role of δ phase in notch sensitivity, the effect of shot peening on LCF life of SHT and MHT materials, and the influence of serrated grain boundaries on LCF and FCGR are addressed.

M. Chang, Department of Mechanical and Aerospace Engineering, Carleton University, Ottawa, Canada; **A.K. Koul, P. Au, and T. Terada,** Structures and Materials Laboratory, Institute for Aerospace Research, National Research Council of Canada, Ottawa, Canada

Table 1 Compositions of experimental alloy 718 materials

Stock type	Composition, wt%								
	Ni	Cr	Nb+Ta	Mo	Ti	Al	Si	C	Fe
Bar	53.2	18.3	5.17	3.0	1.0	0.42	0.12	0.03	bal
Plate	53.1	17.9	5.11	3.06	0.96	0.47	0.21	0.05	bal
Disk	52.5	19.0	5.13	3.05	0.95	0.5	0.35	0.06	bal

Table 2 Heat treatment schedules used and their effect on microstructure

Material	Heat treatment schedule	Average grain size (ASTM No.)	Grain-boundary morphology
SHT	955 °C/1 h/AC + 718 °C/8 h → 1 °C/min → 621 °C/8 h/AC	8/10 (plate/bar)	Planar
MHT	1032 °C/1 h → 3 °C/min → 843 °C/4 h/AC + 926 °C/1 h → 3 °C/min → 718 °C/8 h → 1.6 °C/min → 621 °C/8 h/AC	4/3 (plate/bar)	Serrated
HT2	1032 °C/1 h/AC + 718 °C/8 h → 2 °C/min → 621 °C/8 h/AC	5 (bar)	Planar
Disk	As received (SHT + service exposure)	5-10	Planar
Disk	MHT	5.5	Serrated

Fig. 1 Configuration of DEN specimens
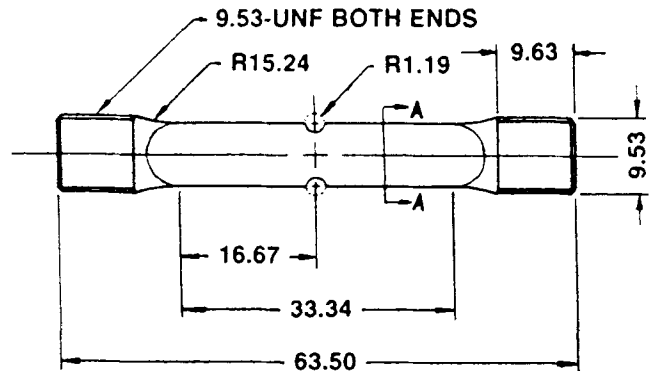
2. Experimental Materials and Test Methods

2.1 Experimental Materials

The commercially available hot-rolled alloy 718 was procured in the form of 22 mm diam bars and 12.7 mm thick by 50.8 mm wide plates. The bar and the plate materials were from two different heats; their chemical compositions are given in Table 1. The bar was used for machining LCF specimens, and the plate was used for machining fatigue crack growth and creep specimens. In addition to the stock materials, a service-exposed turbine disk was procured for machining double-edge-notch (DEN) specimens for notch sensitivity studies.

Each material was examined in the SHT and MHT conditions. The two heat treatment schedules are presented in Table 2, along with the average grain sizes of the bar and the plate materials after SHT and MHT. A selected number of bar and plate specimens were also subjected to another modified heat treatment schedule (HT2) to produce a microstructure similar to MHT but with a planar grain-boundary structure. This was done to elucidate the role of serrated grain boundaries on LCF crack initiation life and FCGR at 650 °C.

2.2 Mechanical Testing

Round creep specimens (4.01 mm diam), conforming to ASTM E 8 specifications, were machined from the heat-treated plate material with the specimen axis perpendicular to the plate rolling direction. Constant-load creep-rupture tests on SHT and MHT materials were conducted at 650 °C in laboratory air at an initial stress of 593 MPa. Creep extension was monitored with a linear variable-differential transformer connected to an extensometer attached to the specimen shoulders.
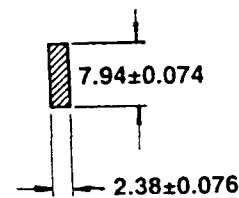
Axial smooth cylindrical LCF specimens (7.62 mm diam), conforming to ASTM E 606 specifications, were machined from the heat-treated bars, and the test section of each specimen was polished manually. Strain-controlled LCF tests were conducted on both SHT and MHT materials at room temperature, 525 °C, and 650 °C, using a triangular waveform and a constant strain rate of 0.002/s at 0.1 Hz and an R value of -1. A few bar specimens subjected to HT2 were also tested at 650 °C to assess the LCF life in the absence of serrated grain boundaries. The yield strength, modulus of elasticity, and hardness of the materials were also measured.

Statistically significant FCGR databases were generated on standard 50.8 mm wide and 12.7 mm thick compact tension (CT) specimens, conforming to ASTM E 647 specifications, at room temperature, 525 °C, and 650 °C in laboratory air. Ten CT specimens, five in the SHT condition and five in the MHT condition, were tested at a given temperature. In addition, four CT specimens, two subjected to MHT and two to HT2, were also tested at 650 °C to quantify the effect of serrated grain boundaries on FCGRs. These four specimens were solution heat treated and aged at the same time in order to obtain similar grain sizes and γ' and γ'' precipitate sizes in all specimens. All CT specimens were precracked at room temperature, and FCGR tests were conducted at an R value of 0.1 and a fre-
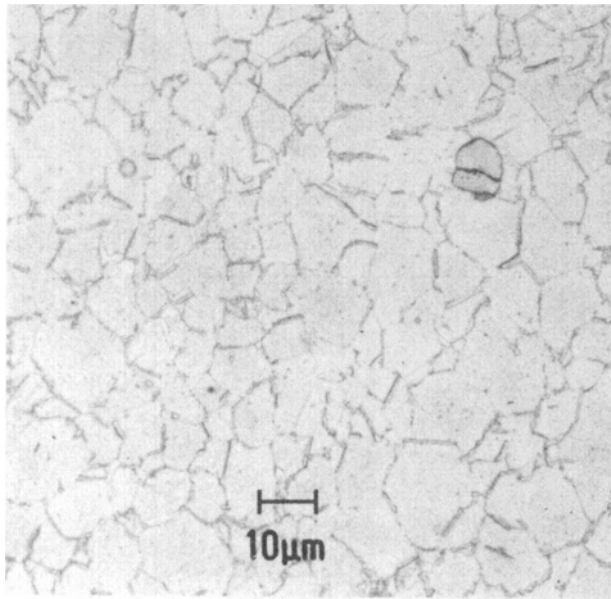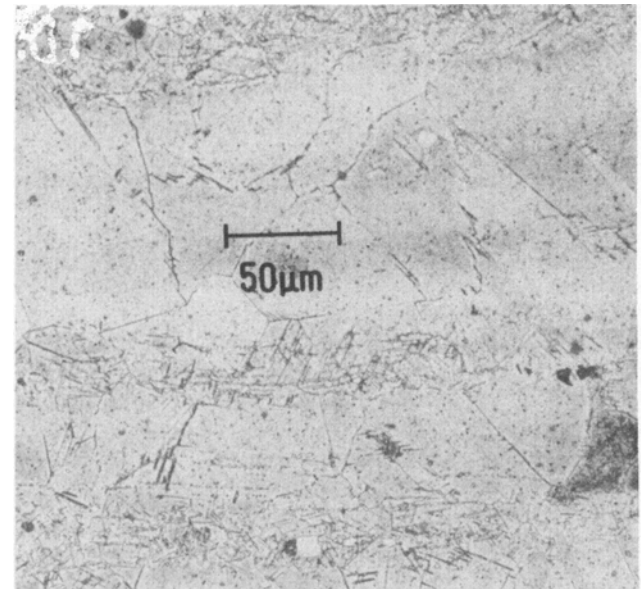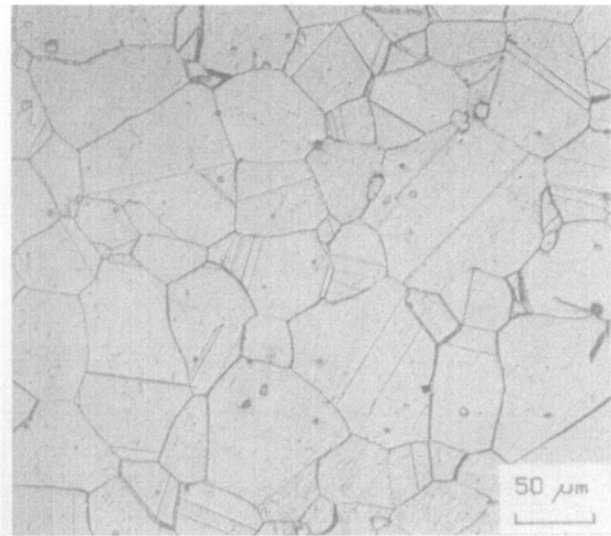
(a)
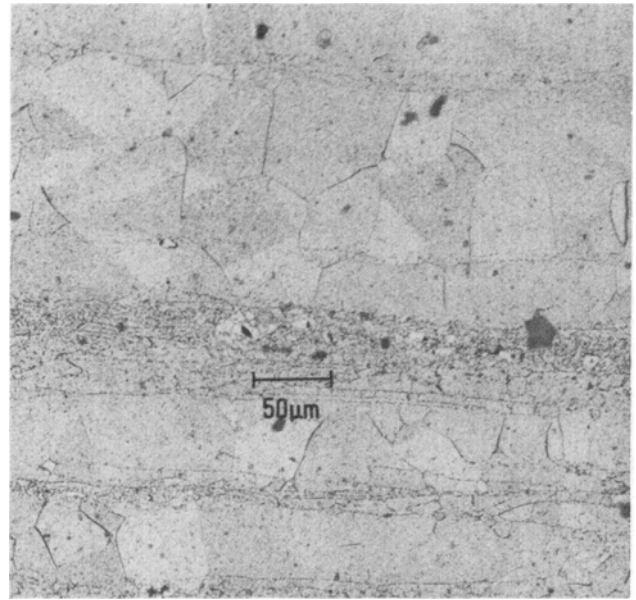
(b)
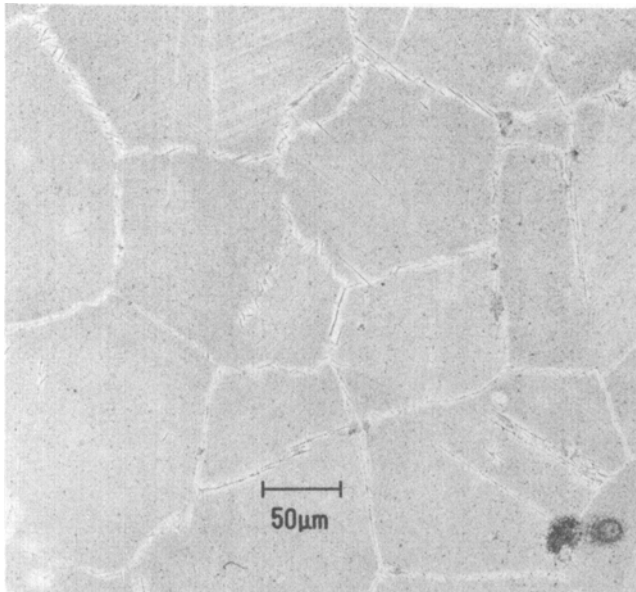
(c)

(d)

Fig. 2 Optical micrographs of the microstructure of alloy 718 bar and plate materials after SHT, MHT, and HT2. (a) Bar, SHT. (b) Plate, SHT. (c) Bar, MHT. (d) Plate, MHT.   (continued)

quency of 1 Hz. The specimen notch was oriented parallel to the rolling direction. A direct-current potential-drop (DC-PD) technique was used to monitor the crack length during FCGR testing.

Six DEN specimens (Fig. 1) were machined from the service-exposed disk; three specimens were subjected to the MHT, and the other three were tested in the as-received condition (when new, the disk had been subjected to the SHT). Machining procedures similar to those used to machine the disk bolt

holes, including drilling and reaming, were used. All specimen surfaces and notch roots were shot peened according to parameters similar to those used to process finished machined disks. The DEN specimens were tested in load control at 650 °C, at a notch root stress of 950 MPa, a frequency of 0.2 Hz, and an R value of 0.1. A high-sensitivity DC-PD technique was employed to detect crack initiation. In DEN specimens, the minimum detectable crack size with this technique is represented by an approximately 0.3 by 0.3 mm quarter elliptical corner crack.

(e)
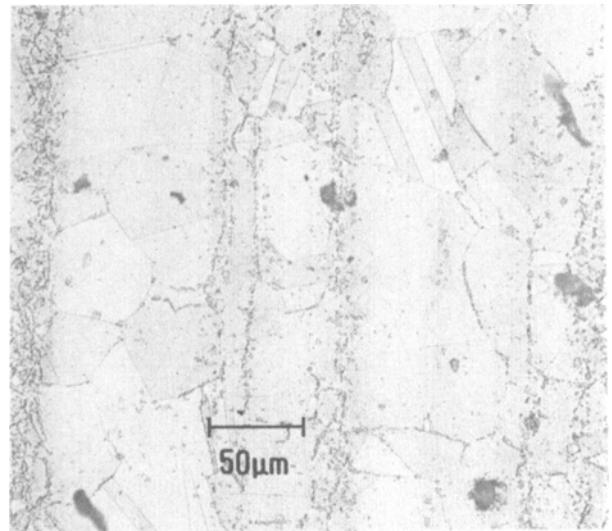
(f)

Fig. 2 (cont.) Optical micrographs of the microstructure of alloy 718 bar and plate materials after SHT, MHT, and HT2. (e) Bar, HT2. (f) Plate, HT2
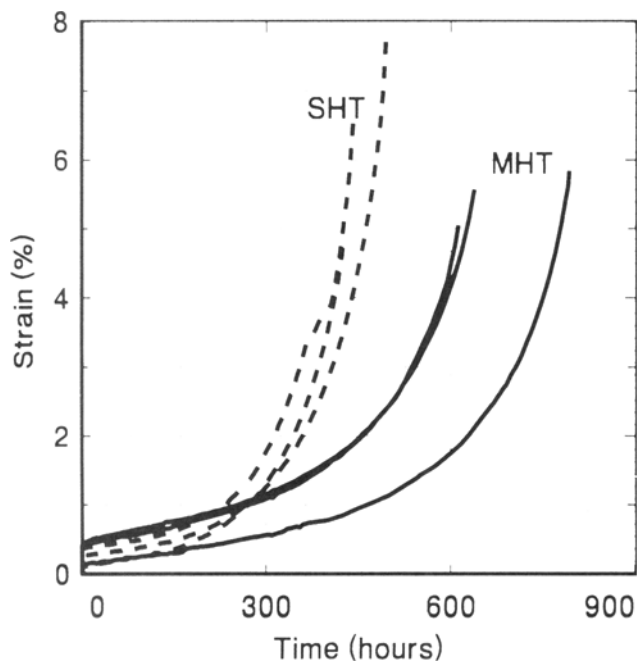

Fig. 3 Constant-load creep curves generated at 650 °C and an initial stress of 593 MPa for SHT and MHT alloy 718

## 3. Results and Discussion

3.1 Microstructures

Optical micrographs showing the microstructures of longitudinal sections of the bar and the plate materials subjected to the SHT, MHT, and HT2 are presented in Fig. 2. The average grain sizes of all materials are compared in Table 2. It is clear that the MHT and HT2 led to an increase in grain size relative

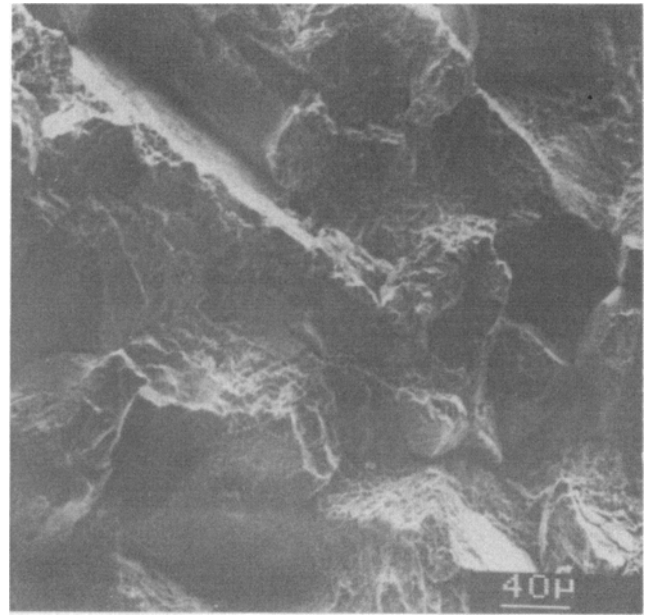**Table 3   Tensile properties of alloy 718**

| Temperature, °C	Heat treatment	0.2% offset yield strength, MPa	Modulus of elasticity, MPa
RT	SHT	1204	198×10^3
	MHT	1036	199×10^3
525	SHT	1066	173×10^3
	MHT	876	172×10^3
650(a)	SHT	970	168×10^3
	MHT	827	168×10^3
	HT2	875	165×10^3

(a) Ref 3

to the SHT. In addition, the MHT produced serrated grain boundaries. The plate material, however, revealed the presence of a heavily banded grain structure; these bands were retained even after the higher solution treatment temperature used in the MHT and HT2 (Fig. 2d and f). Alloy 718 is particularly prone to banded grain structure formation due to inhomogeneous distribution of MC carbides, and these MC clusters help form fine-grained bands in the wrought products. The MHT and HT2 partially modify these banded regions by solutioning some NbC because of a higher solution treatment temperature than for the SHT (1032 versus 955 °C), but a duplex grain size distribution is still retained. In finished forged or rolled products, complete elimination of carbide segregation and duplex grain size formation is possible only if the solution treatment temperature exceeds 1200 °C; however, such a treatment would obviously lead to excessive grain growth. Recent investigations by Poole, Stultz, and Manning (Ref 8) have clearly shown that the banded region in alloy 718 can be eliminated through proper ingot homogenization practice.
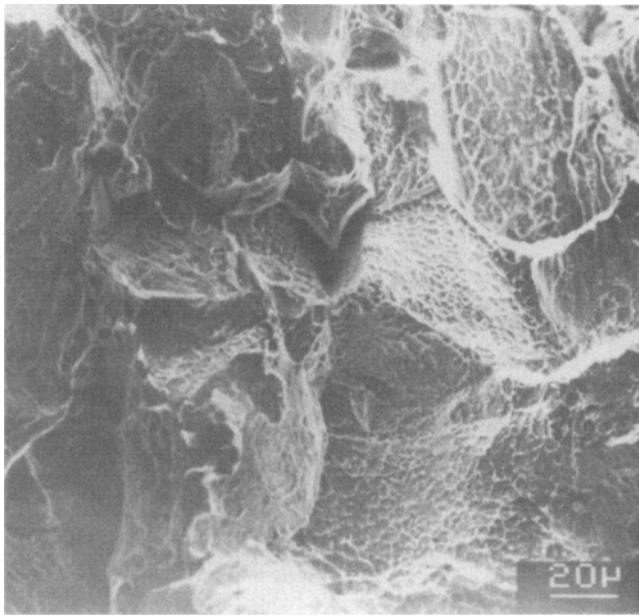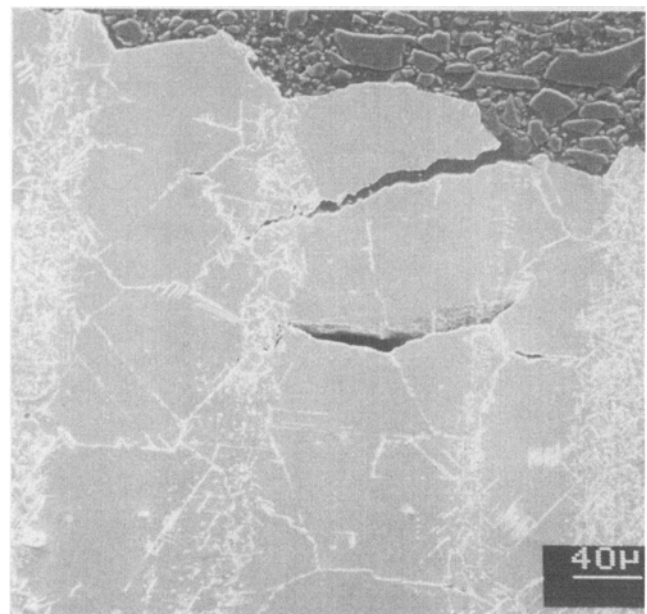
(a)

(b)
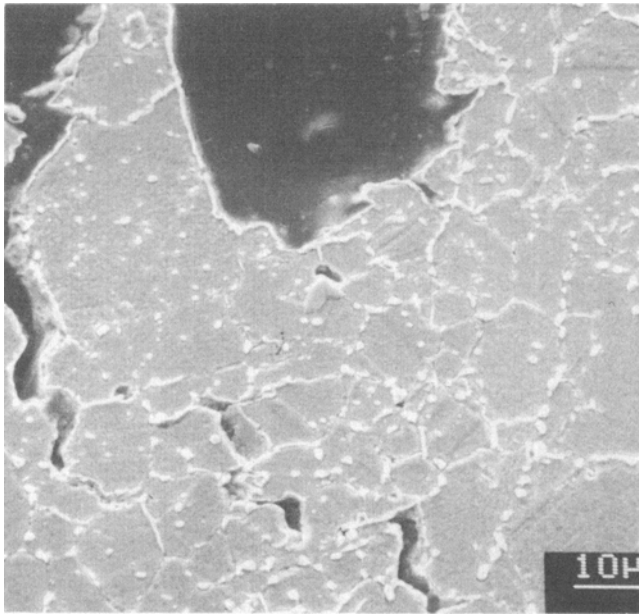
(c)

(d)

Fig. 4 SEM micrographs showing the fracture surface morphology and creep crack paths in alloy 718 creep specimens tested at 650 °C. (a) SHT. (b) MHT. (c) SHT. (d) MHT

3.2 Tensile Properties

The 0.2% offset yield strength and the modulus of elasticity of the SHT, MHT, and HT2 materials are compared in Table 3. These measurements were taken from the first stress-strain cycle during the LCF tests. Relative to the SHT material, the yield strength of the MHT and HT2 materials is lower at all test temperatures, confirming the suggestion made by Antolovich (Ref 4) that the precipitation of grain-boundary δ (orthorhombic Ni_3Nb) phase in the MHT material reduces the amount of ma-

trix niobium content available for γ'' (body-centered tetragonal Ni_3Nb) precipitation. The presence of a coarser grain size in the MHT could also have contributed toward a decrease in yield strength at lower test temperatures through the well-known Hall-Petch effect. The difference in the room-temperature hardness values between the two materials (46.5 HRC for SHT and 44.5 HRC for MHT) is consistent with the yield strength results. The moduli of elasticity of the three materials are comparable at all test temperatures.
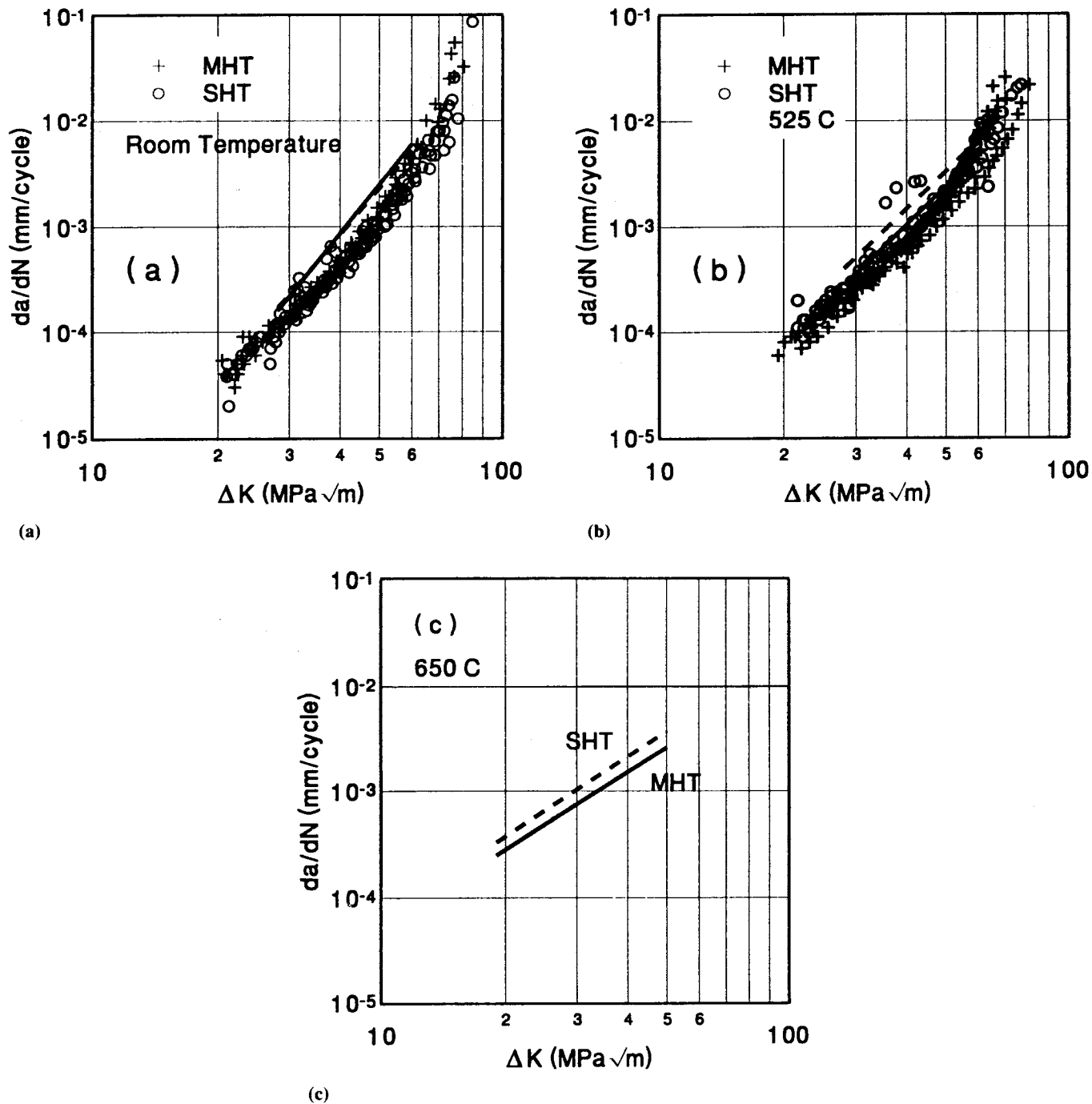
Fig. 5 Fatigue crack growth rate versus stress-intensity range (ΔK) in MHT and SHT alloy 718 materials at (a) room temperature, (b) 525 °C, and (c) 650 °C (upper bound lines only)

3.3 Creep Properties

The creep curves obtained at 650 °C for the SHT and MHT materials are compared in Fig. 3. It is evident that the minimum creep rates in both materials are very similar; however, the MHT improves rupture life by an approximate factor of 1.5 to 2. The life improvement occurs as a result of extended tertiary creep in the MHT material. The creep fracture in the MHT ma-

terial was predominantly transgranular, whereas in the SHT material fracture was primarily intergranular (Fig. 4). These observations indicate that the presence of serrated grain boundaries and a relatively larger grain size suppress grain-boundary sliding in the MHT material and promote transgranular deformation, which leads to an increase in creep life. In Fig. 4(c), it is interesting to note that creep cracks propagate preferentially along the fine-grained regions of the banded structure

Table 4 Comparison of FCGR slopes in Paris regime

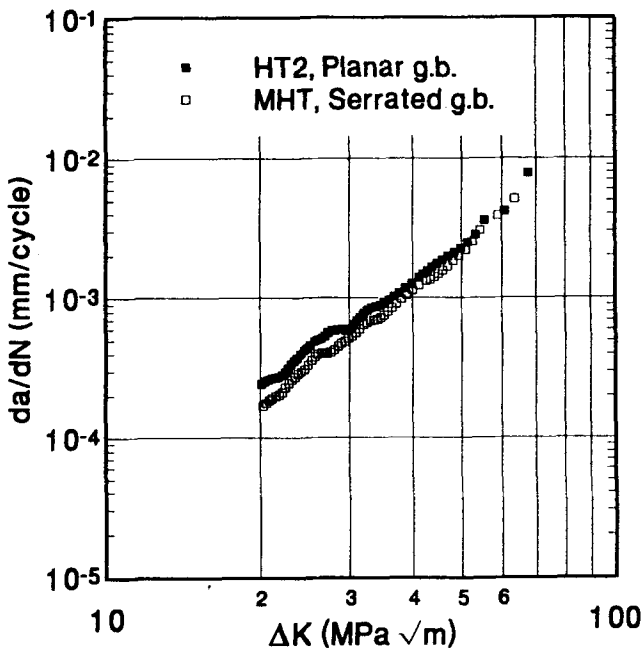| RT		525 °C		650 °C		
MHT	**SHT**	**MHT**	**SHT**	**MHT**	**HT2**	**SHT**
3.99	3.62	3.37	3.18	2.82	2.51	2.53

Fig. 6   Comparison of FCGRs of alloy 718 subjected to MHT (grain size ASTM 4) and HT2 (grain size ASTM 5) tested at 650 °C

in the SHT material. This behavior may also have contributed to the short creep life of the SHT material. The creep fracture strain of the MHT material (5 to 6%) is marginally lower than the creep fracture strain observed in the SHT material (5 to 8%). However, it is difficult to judge the significance of these minor differences because of the limited number of tests (three specimens per material condition) conducted during this investigation.

3.4 Fatigue Crack Growth Behavior

At room temperature the FCGRs of both MHT and SHT materials are similar (Fig. 5a), whereas at 525 °C the FCGRs of the MHT material are lowered by an approximate factor of 2 over the entire Paris regime (Fig. 5b). A trend similar to that observed at 525 °C has previously been reported for the MHT material tested at 650 °C (Fig. 5c) (Ref 1). To determine the statistical significance of these results, the upper bound lines (dashed and solid lines for SHT and MHT materials, respectively, in Fig. 5), representing three conditional standard deviations from the mean lines, are superimposed for comparison. These results further confirm that the MHT is beneficial to alloy 718 FCGRs at elevated temperatures. It is also significant that the MHT does not adversely affect the FCGRs of alloy 718 at room temperature.

Comparison of the FCGRs of the MHT material (serrated grain boundaries) and the HT2 material (planar grain bounda-

ries) at 650 °C in Fig. 6 (two specimens for each case) shows that serrated grain boundaries reduce FCGRs of alloy 718, particularly at lower ΔK values (i.e., 20 to 40 MPa$\sqrt{m}$). The largest difference between the FCGRs of the two microstructures is observed at 20 MPa $\sqrt{m}$. This difference gradually diminishes with increasing ΔK up to 40 MPa $\sqrt{m}$, and above 50 MPa$\sqrt{m}$ the FCGRs of MHT and HT2 materials are identical. This behavior obviously leads to a slightly higher slope within the Paris regime in the MHT material (Table 4). Although both MHT and HT2 materials predominantly fail through an intergranular mode at low ΔK values (Fig. 7a and b), the MHT specimens reveal the presence of a larger area fraction of transgranular fracture, indicating suppression of grain-boundary sliding and promotion of transgranular deformation within the plastic zone. This feature can be attributed to the presence of serrated grain boundaries in the MHT material. At a high ΔK value of 50 MPa$\sqrt{m}$, a mixed transgranular and intergranular fracture is observed in both MHT and HT2 materials, with no significant difference between the two materials (Fig. 7c and d). The influence of serrated grain boundaries on FCGRs in alloy 718 at 650 °C is analogous to the effect of a coarse grain size on the FCGRs where lower crack growth rates are observed at lower ΔK values (Ref 9). Therefore, a combination of coarse grain size and serrated grain boundaries significantly suppresses grain-boundary sliding and markedly improves the fatigue crack growth resistance of the alloy.

The slope (n) values for the Paris regime, where FCGR behavior is represented by $da/dN = C \, \Delta K^n$, are compared for the SHT and MHT materials at room temperature, 525 °C, and 650 °C in Table 4. The n values significantly decrease with increasing temperature for both materials, but, at a given test temperature, the n values for the SHT material are marginally lower than for the MHT material. The observed decrease in n values with increasing temperature is consistent with the results obtained by James and Mills (Ref 10), where n values were observed to decrease from 5.2 at 24 °C to 1.9 at 650 °C, and by Xie (Ref 11) ($n = 3.13$ at 360 °C, 3.03 at 550 °C, and 2.5 at 650 °C). The temperature dependence of n values is perhaps related to the change in the contribution of different deformation mechanisms within the plastic zone toward crack extension and the varying influence of environmental contribution toward crack growth with increasing temperature.

### 3.5 Fatigue Crack Initiation Life in Smooth Cylindrical Specimens

Low-cycle fatigue crack initiation life data, as a function of total strain range, for the MHT and SHT materials are presented in Fig. 8. Previous data, generated at 650 °C (Ref 5), are also superimposed for comparison. The LCF life of the MHT material is generally lower than the SHT material at all test temperatures, but the differences are marked at room temperature. Relative to the SHT material, the LCF lives of the MHT mate-
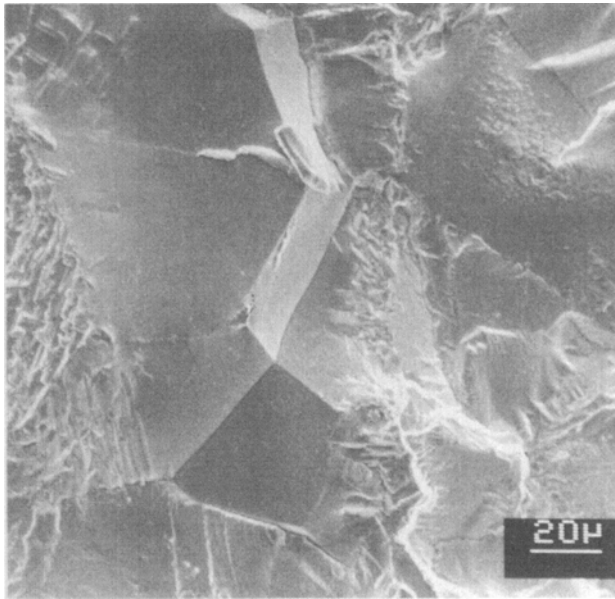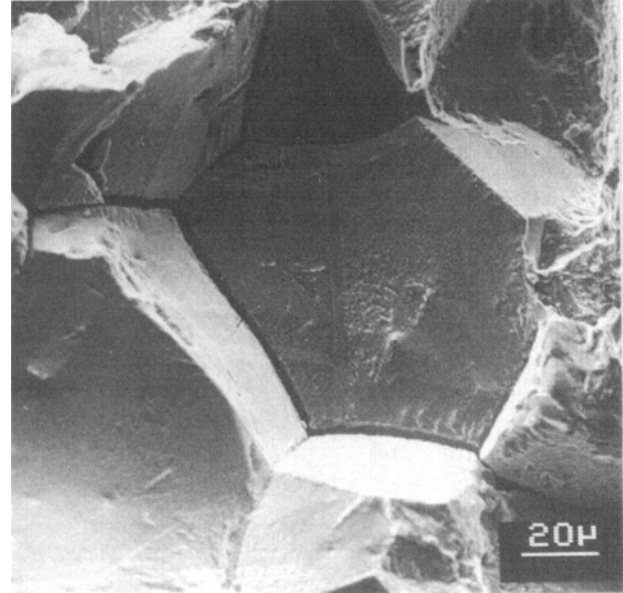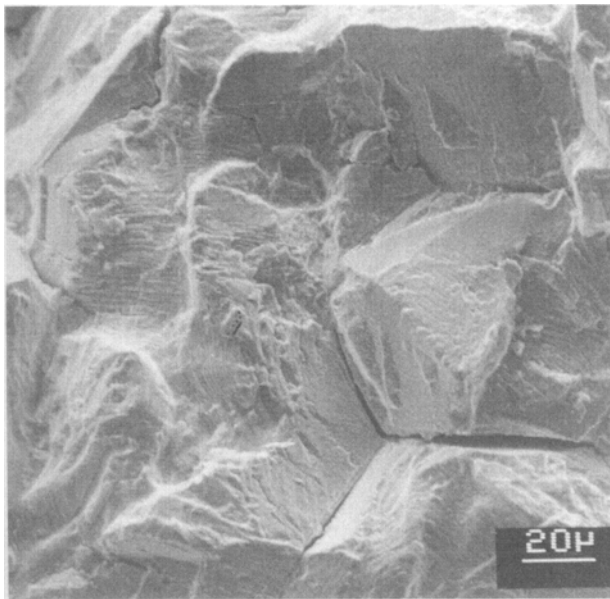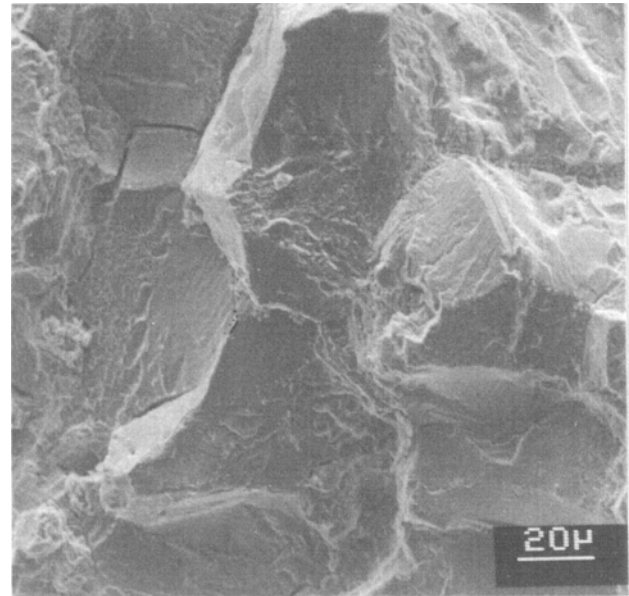
Fig. 7 Fracture morphology of MHT and HT2 alloy 718 materials after FCGR tests at 650 °C. (a) MHT, at 20 MPa√m̄. (b) HT2, at 20 MPa√m̄. (c) MHT, at 50 MPa√m̄. (d) HT2, at 50 MPa√m̄

rial are lowered by factors of almost 3, 2, and 1.5 at room temperature, 525 °C, and 650 °C, respectively. The lower LCF life of the MHT material is most likely related to its lower yield strength, because damage accumulation is greater on a per cycle basis.

A selected number of bar specimens subjected to the HT2 schedule were tested in LCF at 650 °C to evaluate the effect of serrated grain boundaries on crack initiation life. Results comparing the LCF data as a function of total strain range for SHT, MHT, and HT2 materials at 650 °C are shown in Fig. 9. It is clearly evident that the LCF crack initiation lives of the MHT

and HT2 materials are comparable and that, if anything, the serrated grain boundaries lead to a marginal improvement in LCF crack initiation life relative to a planar grain-boundary microstructure in smooth cylindrical specimens.

The monotonic and cyclic stress-strain curves for the SHT and MHT materials are compared in Fig. 10. The HT2 results have not been incorporated because the data were very similar to the MHT data. The MHT material is cyclically more stable than the SHT material at all test temperatures because it initially hardens and then softens marginally, whereas the SHT material softens considerably before stabilizing at a steady-
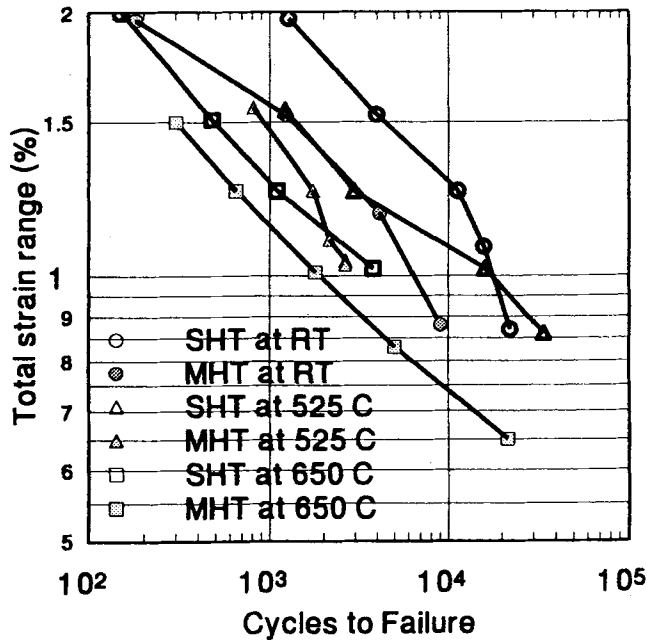
Fig. 8 Low-cycle fatigue crack initiation life results obtained at different test temperatures on the bar specimens ($R = -1$, $f = 0.1$ Hz)
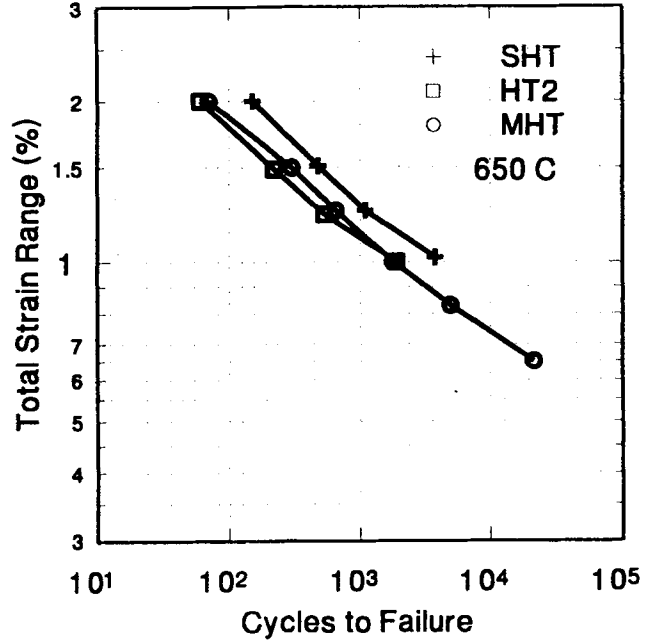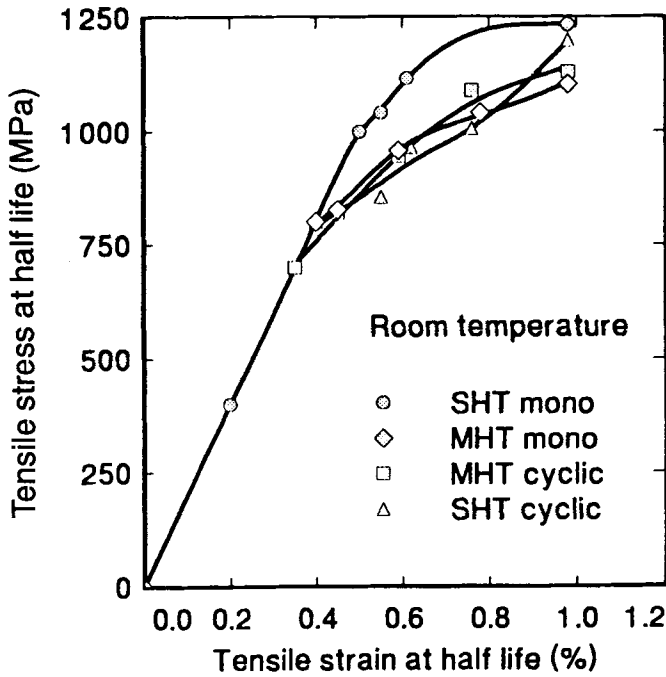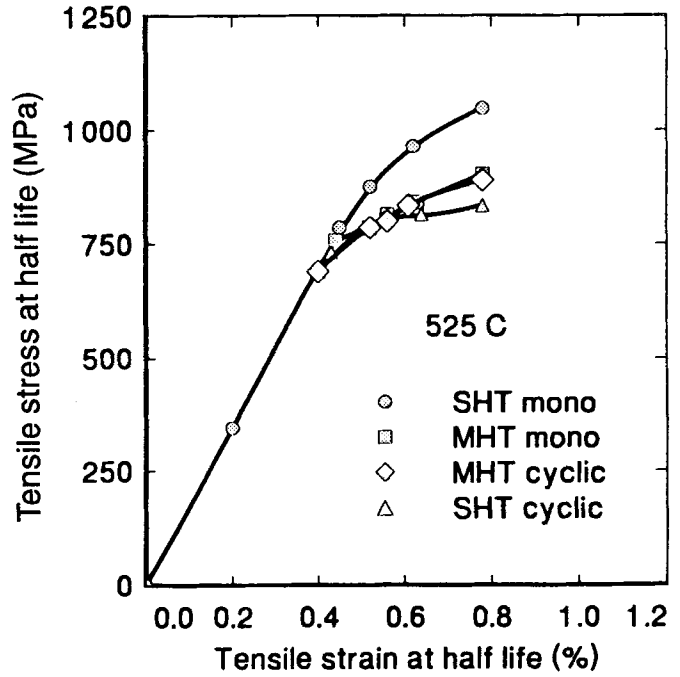

Fig. 9 Low-cycle fatigue crack initiation life comparison of SHT, MHT, and HT2 alloy 718 bar specimens at 650 °C ($R = -1$, $f = 0.1$ Hz)

(a)

(b)

Fig. 10 Comparison of monotonic and cyclic stress-strain response of alloy 718 in SHT and MHT conditions

state stress value. The cyclic softening of alloy 718 in the SHE condition has also been observed by other researchers (Ref 11). The cyclic softening of the standard alloy 718 microstructure (SHT material) is most likely related to the presence of fine γ'' disks, which can lose coherency through interaction with dislo-

cations or be sheared by dislocations during cyclic straining. In contrast, the damage-tolerant microstructure (MHT material) contains a bimodal γ'' distribution where large γ'' precipitates cannot be sheared easily and the loss of coherency is not as severe as for the fine γ'' precipitates. As a result, cyclic softening
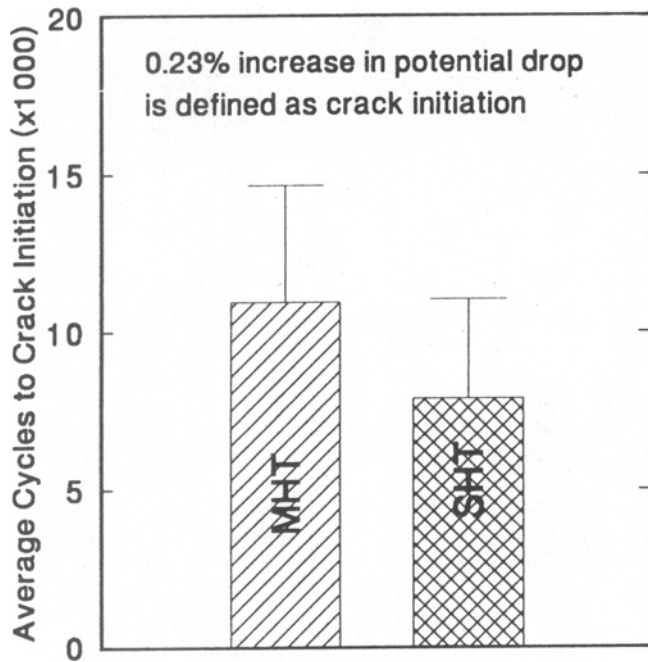
Fig. 11 Comparison of fatigue crack initiation lives of alloy 718 in MHT and SHT conditions in shot-peened DEN specimens tested at 650 °C (average of three specimens for each case).

is not as noticeable in the MHT material as in the SHT material (Ref 5). Cyclic softening of a material is considered deleterious, because the load-bearing capacity of the material is reduced with cyclic strain accumulation.

3.6 Fatigue Crack Initiation Life in DEN Specimens

The DEN specimen testing at 650 °C was undertaken for two reasons: first, to study the relative benefits of shot peening on the LCF crack initiation life of the standard and damage-tolerant microstructures of alloy 718 and, second, to quantify the notch sensitivity of the damage-tolerant microstructure. The average LCF crack initiation lives for three specimens per material condition along with their standard deviations are presented in Fig. 11. The LCF crack initiation life of the MHT material is more than 40% longer than that of the SHT material at 650 °C. Both materials initiated corner cracks (Fig. 12), revealing transgranular but somewhat ductile and faceted fracture morphology in the crack initiation region. This type of fracture morphology often occurs during LCF testing of nickel-base superalloys at elevated temperatures (Ref 12). These results appear to confirm our earlier suggestion that shot peening would leave a deeper compressive residual stress zone in the MHT material due to its lower yield strength (Ref 6). Actual residual stress measurements in the notch root areas of the DEN specimens were not taken, but the results clearly indicate that shot peening is of greater benefit to MHT material than to SHT material. It is also significant that shot peening imparts a beneficial effect on the LCF crack initiation life of the damage-tolerant microstructure at temperatures as high as 650 °C. At such high temperatures some part of the compressive residual stresses would be relieved during the specimen heating and temperature stabilization segment of the crack initiation ex-
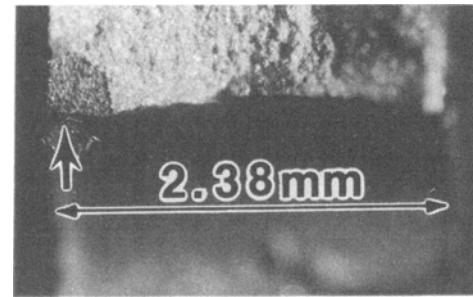
(a)
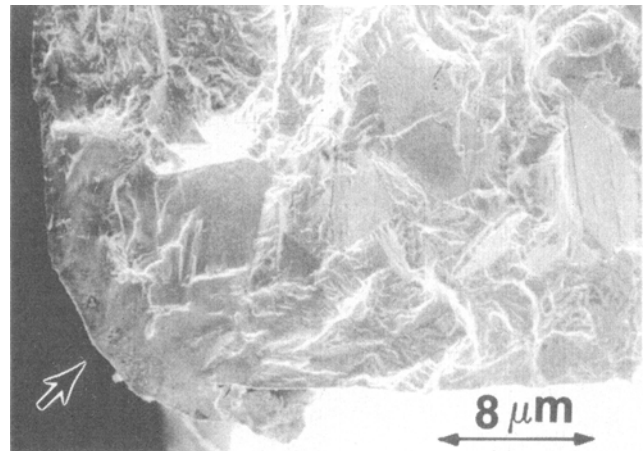
(b)

Fig. 12 Crack initiation morphology of shot-peened alloy 718. (a) Corner crack in SHT material Optical, 21×. (b) Corner crack in MHT material. Note rolling up of the edge. SEM, 250 ×

periment. It is thus expected that shot peening would prove even more beneficial to the fatigue life of the MHT material at lower test temperatures.

The LCF results presented in Fig. 11 also demonstrate that controlled grain-boundary δ-phase precipitation through MHT sequence in wrought alloy 718 material does not make it notch sensitive. Recent work by Benson, Hunziker, and Williams (Ref 13) on alloy 718 diffuser cases from civilian jet engines has revealed that relative to the SHT, the MHT increased the absorbed notch impact energy and decreased the data scatter in dynamic Charpy impact tests conducted at room temperature. Our results, together with those presented in Ref 13, clearly indicate that δ-phase needles precipitated at an angle to the grain boundaries producing a serrated grain-boundary morphology, do not influence the notch sensitivity of alloy 718 material.

Previous results on the high-cycle fatigue (HCF) life of MHT material, where DEN specimens were used in load-controlled fatigue tests at 650 °C, suggested that MHT decreases alloy 718 HCF life (Ref 14). However, in that investigation, the notches in the DEN specimens were machined by lathe, which leaves deep marks on the notch surfaces, or by wire electrodischarge machining, which leaves a thin cast layer on the notch surface. The nature of the cast layer is expected to be microstructure dependent, particularly in the grain-boundary regions. In view of the results obtained for LCF crack initiation

life of the MHT material in shot-peened specimens, it is expected that the HCF life of the shot-peened MHT material will be comparable to that of SHT material. This hypothesis, however, requires further experimental support.

4. Conclusion

Compared to the standard heat treatment, the modified heat treatment changes various mechanical properties of alloy 718 in the following manner:

- It decreases the 0.2% offset yield strength of the material at room temperature, 525 °C, and 650 °C, with no change in the modulus of elasticity.
- It improves creep life by an approximate factor of 1.5 to 2 at 650 °C by extending the tertiary creep life, with no change in the minimum creep rate of the material.
- It decreases the FCGRs by an approximate factor of 2 at 525 and 650 °C over a wide range of ΔK values, with no loss in fatigue crack growth resistance at room temperature. Serrated grain boundaries significantly contribute toward fatigue crack growth resistance at elevated temperatures.
- In strain-controlled LCF tests, it decreases the LCF crack initiation life by factors of 3, 2, and 1.5 at room temperature, 525 °C, and 650 °C, respectively. However, cyclic stress-strain stability of the material is improved at all test temperatures.
- In DEN crack initiation tests on shot-peened specimens, it improves the LCF crack initiation life of alloy 718 material by more than 40%.
- The controlled precipitation of grain-boundary δ phase for producing a serrated grain-boundary structure does not render alloy 718 notch sensitive.

References

1. A.K. Koul, P. Au, N. Bellinger, R. Thamburaj, W. Wallace, and J.-P. Immarigeon, Development of a Damage Tolerant Microstructure for Inconel 718 Turbine Disc Material, *Superalloys 1988*, D.N. Duhl, G. Maurer, S. Antolovich, C. Lund, and S. Reichman, Ed., TMS, 1988, p 3-12

2. D.D. Krueger, R.D. Kissinger, and R.G. Menzies, Development and Introduction of a Damage Tolerant High Temperature Nickel-Base Disk Alloy, René88DT, *Superalloys 1992*, S.D. Antolovich, R.W. Stusrud, R.A. MacKay, D.L. Anton, T. Khan, R.D. Kissinger, and D.L. Klarstrom, Ed., TMS, 1992, p 277-286

3. J.Y. Guedou, J.C. Lautridou, and Y. Honnorat, N18, PM Superalloy for Disks: Development and Applications, *Superalloys 1992*, S.D. Antolovich, R.W. Stusrud, R.A. MacKay, D.L.Anton, T. Khan, R.D. Kissinger, and D.L. Klarstrom, Ed., TMS, 1992, p 267-276

4. S.D. Antolovich, The Effect of Metallurgical Instabilities on the Behaviour of IN718, *Superalloy 718—Metallurgy and Applications*, E.A. Loria, Ed., TMS, 1989, p 647-653

5. H. Bande, Y. Xiao, P. Au, A.K. Koul, and W. Wallace, Low Cycle Fatigue Fracture Behaviour of Conventional and Damage Tolerant Microstructures of Inconel 718 at 650 °C, *Surface Engineering*, S.A. Meguid, Ed., Elsevier Applied Science, 1990, p 238-251

6. M. Chang, A. Au, T. Terada, and A.K. Koul, Damage Tolerance of Alloy 718 Turbine Disc Material, *Superalloys 1992*, S.D. Antolovich, R.W. Stusrud, R.A. MacKay, D.L. Anton, T. Khan, R.D. Kissinger, and D.L. Klarstrom, Ed., TMS, 1992, p 447-456

7. G. Sjoberg, N.-G. Ingesten, and R.G. Carlson, Grain Boundary δ-phase Morphologies, Carbides and Notch Rupture Sensitivity of Cast Alloy 718, *Superalloys 718, 625 and Various Derivatives*, E.A. Loria, Ed., TMS, 1991, p 603-621

8. J.M. Poole, K.R. Stultz, and J.M. Manning, The Effect of Ingot Homogenization Practice on the Structure and Properties of Wrought Alloy 718, *Superalloy 718—Metallurgy and Applications*, E.A. Loria, Ed., TMS, 1989, p 219-228

9. J.P. Pédron and A. Pineau, The Effect of Microstructure and Environment on the Crack Growth Behaviour of Inconel 718 Alloy at 650 °C under Fatigue, Creep and Combined Loading, *Mater. Sci. Eng.*, Vol 56, 1982, p 143-156

10. L.A. James and W.J. Mills, Effect of Heat-Treatment and Heat-to-Heat Variations in the Fatigue Crack Growth Response of Alloy 718, *Eng. Fract. Mech.*, Vol 22(No. 5). 1985, p 797-817

11. J.Z. Xie, Low Cycle Fatigue and Fatigue Crack Growth Behaviours of Alloy 718, *Superalloys 718, 625 and Various Derivatives*, E.A. Loria, Ed., TMS, 1991, p 491-500

12. M. Gell and G.R. Leverant, Mechanisms of High Temperature Fatigue, *Fatigue at Elevated Temperatures*, STP 520, A.E. Carden, A.J. McEvily, and C.H. Wells, Ed., ASTM, 1973, p 37-67

13. J. Benson, R. Hunziker, and C. Williams, Rejuvenation of Wrought IN-718 Diffuser Cases, *Superalloys 1992*, S.D. Antolovich, R.W. Stusrud, R.A. MacKay, D.L. Anton, T. Khan, R.D. Kissinger, and D.L. Klarstrom, Ed., TMS, 1992, p 877-883

14. R.G. Andrews, A.K. Koul, and P. Au, Fatigue Crack Initiation in Alloy 718 at 650 °C, *Superalloys 718, 625 and Various Derivatives*, E.A. Loria, Ed., TMS, 1991, p 943-954